JOURNAL OF CATALYSIS 82, 442–456 (1983)

Evolution of Surface and Bulk Compositions of an Iron Catalyst in Relation to Catalytic Activity for the Fischer–Tropsch Reaction

D. BIANCHI,* S. BORCAR,† F. TEULE-GAY,‡ AND C. O. BENNETT§,[1]

*UER Chimie, University of Lyon, Villeurbanne, France; †Texaco, Port Arthur, Texas; ‡Institut Français du Pétrole, Rueil-Malmaison, France; and §Department of Chemical Engineering, University of Connecticut, Storrs, Connecticut 06268

Received January 7, 1982; revised February 22, 1983

During the initial period of exposure of a reduced 10% Fe/Al_2O_3 catalyst to 10% CO/H_2 at 1 atm and 285°C, the surface and bulk compositions of the iron crystallites are observed. The bulk composition is determined by Mössbauer effect spectroscopy. The surface composition is deduced from transient experiments during which the gas analysis is followed by mass spectroscopy. After about 30 min of exposure to the reaction mixture three surface species are detected: a reactive species (50 μmol/g); a less reactive species (226 μmol/g); and an inert species (50 μmol/g). These surface species do not contain oxygen. It is probable that their differences in reactivity are due to differences in chemical nature (hydrogen content) and they are not merely different forms of carbon. After 30 min time the bulk of the iron is about 74% carburized to a mixture of χ-$Fe_{2.5}C$ and ε'-$Fe_{2.2}C$.

INTRODUCTION

One of the principal problems in understanding the Fischer–Tropsch synthesis over iron-based catalysts is a lack of knowledge of the relation between the rate of reaction and the composition of the catalyst. For iron, more than most other typical catalyst metals, both the surface and the bulk compositions change slowly, associated with slow changes in catalytic activity. In this work, we consider the activity and composition changes over the first 100 min of time on stream. This time is much greater than that associated with the life of active centers which lead to the observed production rates (turnover frequencies) of hydrocarbons.

For iron catalysts, the activity of a freshly reduced catalyst increases from an initial low value to reach a maximum after an hour or less (*1–3*); at higher times on stream, the reaction rate then slowly decreases. The deactivation process has been the subject of a number of studies (*1–5*), and it is generally assumed that the deactivation is related to the deposition of inactive carbon (graphite) on the surface of the solid. Studies of the initial increase show a correlation between the degree of carburization and the catalytic activity of the iron (*1–4*). One explanation claims that iron carbide is a better catalyst than metallic iron (*1, 2*), whereas another purposes that the reaction intermediate (active carbon) which leads to hydrocarbon formation leads also the carbide (*3, 4*). As the iron carbide builds up toward saturation, the concentration of intermediate increases, leading to a higher reaction rate. Such studies measure bulk compositions by x-ray diffraction (*3*) or Mössbauer effect spectroscopy (*1, 2, 4, 5*).

Surface studies during the initial period have made use of Auger electron spectroscopy or x-ray photoelectron spectroscopy, using ultra-high vacuum and metallic films or single crystals (*6, 7*). It has been shown that iron is rapidly covered by a carbonaceous layer which is more or less hydroge-

[1] To whom all correspondence should be addressed.

0021-9517/83 $3.00

nated and that inert graphite also builds up (*6*). The present work is aimed at the study of the surface and the bulk of a conventional iron catalyst supported on alumina during the initial reaction period.

In the work presented here the bulk composition of the iron is followed by Mössbauer effect spectroscopy (MES). An appropriate *in situ* cell is used. The surface compositions are investigated by the use of the transient method, with mass spectrometry to determine gas-phase compositions (*3*). The rates of product formation are followed after a switch to 10% CO/H_2 at 250–300°C and 1 atm over an initially well reduced catalyst.

After various times on stream the surface and bulk species are removed by a switch from reaction mixture in the feed to pure hydrogen (*3*).

EXPERIMENTAL

Materials

The catalyst used in this work is 10% by weight iron on Al_2O_3 (Alon C) obtained by the precipitation method from a solution of $Fe(NO_3)_3 \cdot 9H_2O$ (*5*). To a suspension of Al_2O_3 in this solution at 70°C is added a solution of Na_2CO_3 at the same temperature. The slurry is boiled for 5 min and the resulting solid is filtered and washed. After drying at 120°C for 24 h, the solid is ground to a fine powder of BET surface 105 m^2/g, close to the original area of the support (110 m^2/g). The catalyst is then reduced for all the experiments described here. It is first treated at 250°C in helium for 1 h, and then heated in flowing hydrogen in the reactor to 460°C and reduced for 15 h at 460°C.

The gases used in the study were of high purity grade. They were used without purification except by passage through a tube heated to 250°C to decompose any metal carbonyls present.

Characterization of the Catalyst

The metallic surface of the catalyst was investigated by several experiments involving chemisorption. For CO it has been assumed that there are two surface atoms per molecule of CO, corresponding to linear adsorption with stearic effects (*8*). In associated infrared studies (*9*) we find that a catalyst disk reduced as described here shows a strong band at 2020 cm^{-1}, characteristic of linearly adsorbed CO (*10*). No bridged CO is apparent. For hydrogen, a ratio of 2 iron atoms per molecule of H_2 has been used. To calculate iron surface areas and the equivalent diameter of spherical particles, an average iron atom surface area of 8.2 $Å^2$ has been used (*11*). The following results were obtained.

1. Pulsed chemisorption of pure CO at 25°C. The chemisorption measured is 20 μmol CO/g catalyst, leading to a particle size of 425 Å, or 1.97 m^2/g of catalyst. This value compares with 21.5 μmol/g for 15% Fe/Al_2O_3 found by Vannice (*12*) and 1.96 mol/g of 8.5% Fe/Al_2O_3 found by Brenner and Hucul (*13*), both by chemisorption of CO at 25°C.

2. Static chemisorption of CO at 25°C in a volumetric apparatus. This experiment gave essentially the same results as the pulse method: 17.3 μmol/g catalyst, leading to 491-Å particles. The results have been corrected for reversible adsorption effects.

3. Static chemisorption of CO at −74°C, as in 2. This study gives an adsorption of 63 μmol/g catalyst, leading to 135-Å particles.

4. Hydrogen adsorption at temperatures above 100°C, by the method of Amelse et al. (14). In this method the reduced catalyst is exposed to H_2 at 460°C and then slowly cooled in H_2 to 0°C. The activated adsorption of H_2 increases along its isobar as the temperature decreases. Below a certain temperature (>0°C) the adsorption ceases as its kinetics becomes too slow. The amount of hydrogen adsorbed is then determined by temperature-programmed desorption. For our 10% Fe/Al_2O_3 catalyst this method gives 34 μmol H_2/g catalyst, or 248-Å particles. Amelse *et al.* (*14*) for 9.33% Fe/SiO_2 obtained 24.7 μmol/g and thus 340 Å.

From the foregoing results it is clear that chemisorption leaves us uncertain about the dispersion of the catalyst. This is so not only because of the uncertain ratio of adsorbate to Fe but also because of lack of knowledge of the adsorption isobars and isotherms. For hydrogen, the isobar was determined in 1935 (*15*). It is not known whether the maximum in the isobar is a result of a kinetic cutoff or because of monolayer formation, as one might hope. We experimented further and find that holding the catalyst in H_2 at 100°C for lengthening periods before desorption increases the quantity desorbed. In a recent work, Jung *et al.* (*16*) discuss at length various ways of using CO chemisorption to measure dispersion, but no definitive solution to the problem is offered. However, chemisorption at −78°C is favored by these authors. Boudart *et al.* (*17*) were able to get agreement between particle sizes measured by chemisorption, electron microscopy, and x-ray diffraction for Fe/MgO catalysts by using CO chemisorption at −80°C.

For fused iron catalysts, Solbakken *et al.* (*18*) recommended CO adsorption at either −196 or −78°C, for which equivalent results were obtained, providing that certain procedures were followed. They used a Fe/CO ratio equivalent to about 2. This method has been used by us previously for measuring the iron part of the surface of promoted fused iron catalysts (*3*).

These three studies of iron in different environments do seem to agree that CO adsorption at −78°C leads to values consistent with other measurements.

Our reduced 10% Fe/Al_2O_3 catalyst was studied by x-ray diffraction, and from the extent of line broadening the crystallite particles have a diameter of 160 Å. Transmission electron microscopy (TEM) indicates a mean particle size in the range 160–200 Å. Before reduction, the MES analysis indicates that the iron is present as α-Fe_2O_3. After reduction, the iron is present as 76% Fe^0 and 24% Fe^{2+}, irreducible for our conditions. This lack of complete reduction is in accord with previous results (*1, 2, 4, 5*). More details of our Mössbauer studies on this matter are given in a later section.

These results, leading to a particle size in the order of 160–200 Å, appear to agree best with our CO chemisorption results at −74°C. If the results already mentioned (135 Å) is corrected for the measured 76% degree of reduction to Fe^0, it becomes 173 Å. Thus for our work also, chemisorption at dry-ice temperature seems to agree with XRD and TEM measurements.

Using about 100 μmol iron sites/g catalyst, our rates, given in what follows as μmol/min g catalyst, can be transformed into turnover frequencies in s^{-1} by dividing by 100 and by 60.

Mössbauer Reaction System

Transmission spectra were obtained in the constant acceleration mode with an Elscinct Mössbauer spectrometer. The 14.414-Kev Mössbauer radiation was obtained from a 85 mCi $^{57}Co/Pd$ source (New England Nuclear). The hyperfine spectrum of a 12.5-μm Fe foil was used to provide a linearity check and to define a zero for isomer shift calculations. The outer lines of the six-peak Fe^0 spectrum (line width 0.23 mm/s) were used for velocity calibrations. Lorentzian profiles were used to fit the series of MES resonance spectra by the method of minimizing the values of the sum of the squares of the deviations between the experimental points and the calculated points. The spectra was fitted by using the University of Connecticut IBM 360 computer and the flexible least squares routine of Wilson and Schwartzendruber (*19*).

A stainless steel Mössbauer transmission cell with beryllium windows was used for *in situ* catalyst treatment (*20*). Heating was accomplished by using four cartridge heaters capable of heating the catalyst sample pellet to 500°C at a rate of 1°C/s. A copper jacketed air circulator was used to cool the windows and to cool the cell after temperature treatments. A controlled gas environment (1 atm) of any desired gas mixture

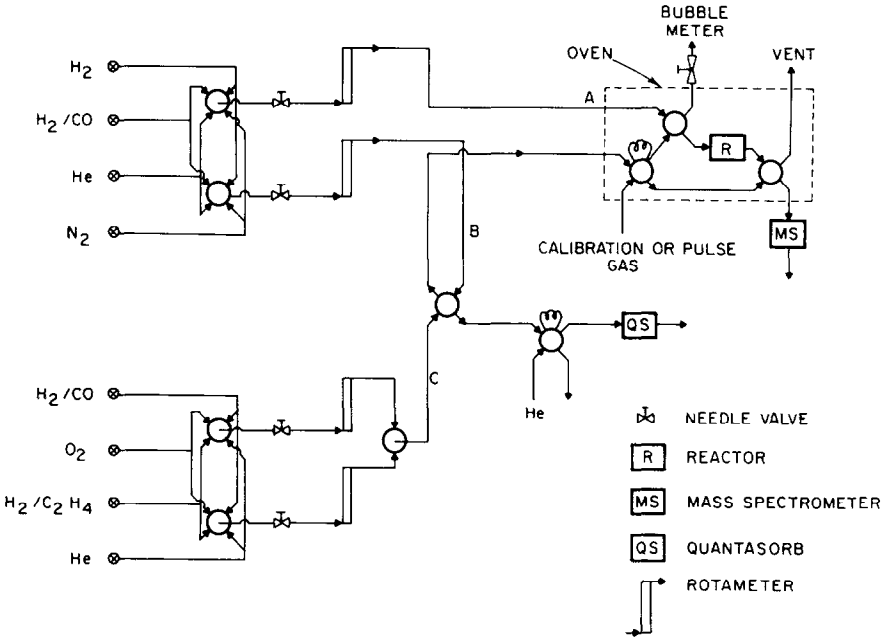

FIG. 1. Flowsheet for the transient experiments.

could be maintained inside the cell at isothermal conditions for controlled time periods. After treatment, the cell was rapidly cooled, and the Mössbauer spectra were recorded at room temperature.

The catalysts pellet used in the cell weighed 250 mg. The inlet and outlet of the cell were connected to a thermal conductivity detector so that a qualitative indication of reaction could be obtained. The space velocity was adjusted to be the same as that used in the kinetic experiments to be described next.

Extensive MES studies have been made and are reported in a separate paper (*21*), which contains details of the equipment, the computer fitting procedure, the calibration methods, and the interpretation of the spectra.

Mass Spectrometer Reaction System

A cycloidal mass spectrometer, Model CEC 21621, was used with a classical continuous inlet system designed for fast response (2 s) and for the avoidance of mass fractionation. The flow sheet (Fig. 1) has been described (*3*). Some of the gases indicated in Fig. 1 were not used in this particular study. By a suitable arrangement of switching valves the composition of the gas flowing to a differential reactor (51.8 mg of catalyst, 33 ml/min gas flow at ambient conditions in a bed of 0.01 ml gas volume) could be suddenly changed, for example, from H_2 to He to 10% CO/H_2 to He to H_2. These step change of the composition of the gas entering the reactor produce responses in the composition of the gas leaving the reactor which were followed by the mass spectrometer via the continuous inlet system.

The powdered catalyst was too finely divided for use in the reactor, so it was lightly compressed into a disk. This was then fragmented and screened so that the particles were in the size range 590 to 840 μm. This particle size was small enough to prevent internal composition gradients and large enough to produce a reasonably low pressure drop.

The analysis of the products of reaction by gas chromatography (flame ionization

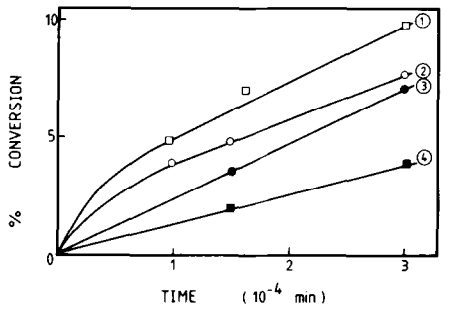

FIG. 2. Effect of contact time on conversion of CO at 270°C, for 52.8 mg of 10% Fe/Al_2O_3. (1) Total conversion of 10% CO/H_2. (2) Conversion of 10% CO/H_2 to hydrocarbons. (3) Total conversion of 10% CO/H_2 saturated with water at 19°C. (4) Conversion of 10% CO/H_2 saturated with water at 19°C to hydrocarbons.

detector) (*22*) indicated that no olefins appear in the products for the conditions used here: 10% CO/H_2, 250–300°C, 1 atm. Paraffins through C_4 are observed, so the peaks chosen for following the composition by mass spectrometry were 15, 18, 27, 28, 29, 43, and 44. The composition data obtained at the outlet of the differential reactor were used with the flow rate and the mass of catalyst to calculate the reported rates of production (μmol/min g of catalyst) for CH_4, C_2H_6, C_3H_8, C_4H_{10}, CO_2, and H_2O. The mass spectrometer output is essentially continuous in time, but points are shown in some figures merely to identify the various curves.

RESULTS AND DISCUSSION

Evolution of the Rate of the CO/H_2 Reaction

Figure 2 shows the conversion of CO as a function of space time at 270°C, measured after a time on stream (after a switch from H_2 to 10% CO/H_2) of 20 min. As previously reported for a fused iron catalyst (*23*), there is not a linear relation between conversion and space time (curves 1 and 2). However, if the feed to the reactor is saturated with water at 19°C, the linear relation expected for a differential reactor is obtained (curves 3 and 4). The well-known inhibiting effect of water is thus confirmed. If water is added as above to the feed gas for a system operating at a point on curve 1, the conversion jumps down to a point on curve 3. When the water is removed, the conversion jumps back to its original level on curve 1.

We next discuss data obtained at a fixed space time (3×10^{-4} min) in the period following a switch from hydrogen flowing over a well reduced catalyst (H_2 at 460°C) to a flow of 10% CO/H_2. This mixture can be introduced in several ways, as discussed in what follows.

When a switch is made directly from H_2 to 10% CO/H_2 at 270°C, the reaction rates shown in Fig. 3 are obtained. The rate of production of C_2^+ hydrocarbons goes through a flat maximum at 20–60 min and then decreases slowly up to 3 h, the longest time used here. Unlike the other products, CH_4 is produced at a very high rate initially. Figure 4 shows the first minute of reaction in detail; for the first 8 s only methane is produced. As we shall see later, carbonaceous intermediates are accumulating on the catalyst surface very rapidly during the initial 20–30 s.

When a switch is made from H_2 to He, either at 460°C or at reaction temperature, hydrogen is desorbed rapidly. A standard period of 40 s helium contact has been used in certain experiments, a time largely sufficient for the desorption of hydrogen at about 270°C. A subsequent switch from He to 10% CO/H_2 gives the results for CH_4 and C_2H_6 shown also in Fig. 4. The initial peak of methane is much reduced, and the higher hydrocarbons appear immediately; the water curve is not changed. After the first minute the curves rejoin those obtained without the intermediate helium treatment. The possibility that oxygen or water in the helium is deactivating the catalyst was considered. The addition of a liquid nitrogen trap to the helium line did not alter the results, nor did a change in helium purge time from 10 to 30 or 60 s.

With the direct switch from H_2 to 10% CO/H_2, the large excess of hydrogen on the surface accounts for the large initial meth-

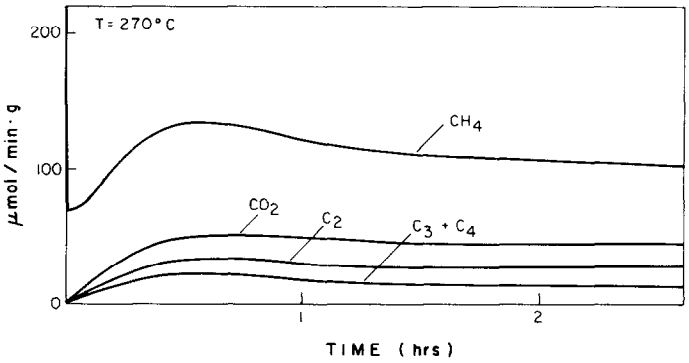

FIG. 3. Production rates at 270°C after a switch from H_2 to 10% CO/H_2.

ane peak. The rate of chain growth is slow compared to the direct hydrogenation of the surface carbonaceous intermediate. Higher hydrocarbons, water, and CO_2 appear only after 8 s. The coincidence of the production of water and higher hydrocarbons has been mentioned by Nijs and Jacobs (*24*) for a cobalt catalyst. However, when the switch $H_2 \rightarrow$ He $\rightarrow$ 10% CO/H_2 is made, Fig. 4 shows that C_2H_6 (and also $C_{3,4}$; not shown) is produced immediately, with the CH_4. Water and CO_2 are still delayed 8 s. Thus it is probable that the higher hydrocarbons are produced because there is relatively less hydrogen on the surface and not because of the presence of water. The later appearance of both water and CO_2 is explained by their adsorption on the alumina support which had come directly from its treatment under H_2 at 460°C. We have found that Al_2O_3 dried at 460°C can adsorb 450 μmol/g of water at 270°C.

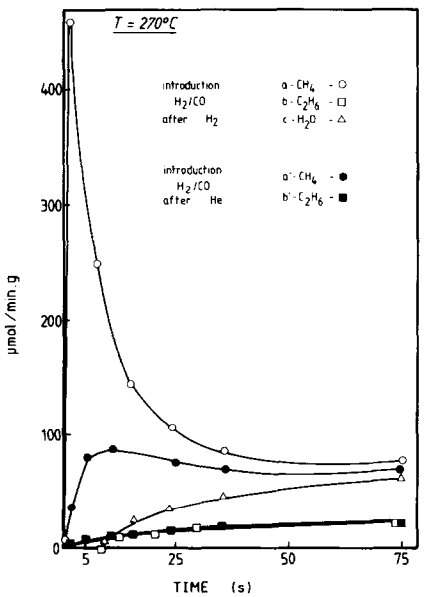

FIG. 4. Reaction rates without desorption of H_2 after $H_2 \rightarrow$ 10% CO/H_2 (unfilled symbols). Reaction rates with initial desorption of H_2 after He $\rightarrow$ 10% CO/H_2 (filled symbols).

The initial reaction period has been studied by other authors (*1, 5*) who used gas chromatography for analysis. Their curves resemble Fig. 3, but without the initial methane peak and the other details shown in Fig. 4. Thus a natural explanation of the increase in activity with time is that iron carbide, being formed during the period of Fig. 3, is the catalyst and that iron is not active. Our results show that iron is a good catalyst but that its surface is rapidly altered so that its activity is greatly lowered. At longer times (up to 30–60 min) the activity rises slowly; in what follows we explore this behavior by means of our measurements of the surface and bulk composition during the period covered by Figs. 3 and 4.

Note that Matsumoto and Bennett (*3*) would have observed the initial CH_4 peak, had it existed for their fused iron CCI catalyst. This difference will be discussed further in future work.

Experiments analogous to those of Fig. 3 have been done at 250, 270, and 285°C,

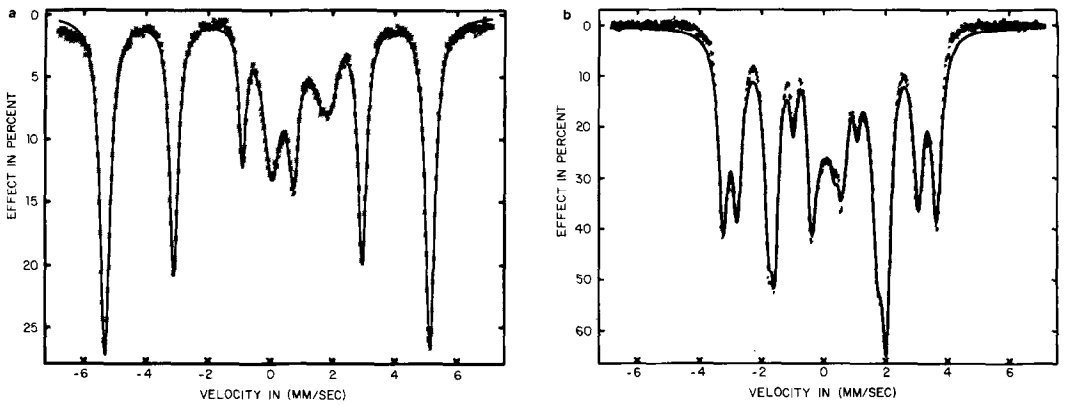

FIG. 5. (a) Mössbauer spectrum of 10% Fe/Al_2O_3 catalyst after reduction at 460°C for 17 h. (b) Mössbauer spectrum of 10% Fe/Al_2O_3 catalyst after reduction and carburization in 33% CO/H_2 at 390°C.

without preliminary desorption of H_2. The activation energy based on both the rate at the initial maximum point and after 10 min is 20.4 kcal/mol, a value comparable to that of previous studies; 23.0 kcal/mol (*7*); 21.3 kcal/mol (*12*). This remarkable constancy of the activation energy at these two times indicates that the rate-controlling step is probably the same at both instants. The selectivity for CH_4 after 10 min, defined as the rate of CH_4 production divided by that of the sum of the rates of all the hydrocarbons, is 52%, close to the value found by Vannice (*12*), estimated from his data for $H_2/CO = 15$.

Evolution of the Catalyst Bulk with Time Studied by Mössbauer Effect Spectroscopy

As mentioned previously, details of the Mössbauer studies are to be presented separately (*21*). Here a few results are given to show the quality of the spectra and to support the interpretation of some of the results obtained by mass spectrometry. Niemantsverdriet *et al.* (*4*) have shown that during the CO/H_2 reaction over iron, the metal is carburized principally to a mixture of χ-$Fe_{2.5}C$ and ε'-$Fe_{2.2}C$. We find a similar result (*21*).

Figure 5a shows the spectrum of our reduced catalyst (H_2, 450°C, 17 h). The two outer lines on each side agree in position and intensity ratio with the lines obtained from the standard iron foil. Five-hundred and twelve velocity channels have been used. The two inner Fe^0 peaks are distorted by additional peaks. When the two inner peaks for Fe^0, which have intensities and line widths fixed by their nature, are subtracted out, there remains in the central part of the spectrum a four-peak spectrum which can be associated with Fe^{2+}. The Mössbauer parameters are reported in Table 1, where the values are given for Fe^0 and Fe^{2+} for the reduced catalyst. This catalyst is 74% Fe^0 and 26% Fe^{2+}.

It is not possible to find carburizing conditions which lead to pure ε'-$Fe_{2.2}C$, but approximately pure χ-$Fe_{2.5}C$ can be obtained by treatment at 390°C by 33% CO/H_2 for 24 h. Figure 5b shows the resulting spectrum. Only peaks corresponding to the χ-form are visible, as identified by Niemantsverdriet (*4*). The spectrum is made up of three hyperfine spectra of six peaks each plus four mostly hidden peaks of Fe^{2+}. Table 1 gives the line positions, Mössbauer parameters, and the ratios of the peak areas in each individual hyperfine field, and the ratios of the areas corresponding to the three fields themselves.

Figure 6 shows the spectrum of the catalyst carbided at 270°C for 24 h in 10% CO/

TABLE 1a

Mössbauer Parameters of Fe Species Detected over 10% Fe/Alon C at Room Temperature (298°K)[a]

Treatment	Species	Spectral contribution[b] area (%)	Isomer shift (mm/s) δ	Quadrupole splitting (mm/s) ΔE_Q	Hyperfine field (kOe) H
Catalyst after the reduction sequence (Fig. 5a)	Fe^0	76	0.0	0.0	330
	Fe^{2+}(A)	24	1.12	1.02	0.0
	Fe^{2+}(B)		1.08	0.64	0.0
Catalyst carburized at 390°C, (Fig. 5b) χ(I):χ(II):χ(III) = 2.14:2.35:1	χ-$Fe_{2.5}C$ (I)	86	0.22	0.11	183
	(II)		0.26	0.14	219
	(III)		0.17	0.08	106
	Fe^{2+}(A)	14			
	Fe^{2+}(B)				
Catalyst carburized at 270°C (Fig. 6) χ(I):χ(II):χ(III) = 2.52:2.77:1	χ-Fe_5C_2 (I)	24			
	(II)				
	(III)				
	ε'-$Fe_{2.2}C$	63	0.24	0.11	171
	Fe^{2+}(A)	13			
	Fe^{2+}(B)				

[a] Isomer shift data reported with respect to α-Fe.
[b] The recoil-free fraction is assumed equal for all species.

TABLE 1b

Some Details of the Mössbauer Effect Spectra[a]

Sample	Center of the peaks, channel number[b]						Area ratios					
Fe^0 (Fig. 5a)	57,	138,	219,	278,	359,	439	3.30,	2.13,	0.93,	1.00,	1.96,	3.05
χ-Fe_5C_2 (I)	151,	190,	240,	271,	320,	363	3.06,	1.97,	1.18,	1.00,	2.07,	3.06
(Fig. 5b) (II)	132,	186,	236,	277,	327,	386	2.96,	1.95,	1.11,	1.00,	1.81,	2.95
(III)	193,	215,	244,	266,	291,	315	3.26,	1.93,	1.00,	0.94,	1.96,	3.28
χ-Fe_5C_2 (I)							2.99,	1.94,	1.00,	1.04,	1.99,	2.99
(Fig. 6) (II)	The same as Fig. 5b						3.07,	2.01,	1.00,	0.96,	2.06,	3.07
(III)							2.85,	2.02,	1.00,	1.14,	1.79,	2.91
ε'-$Fe_{2.2}C$ (Fig. 6)	159,	199,	240,	272,	313,	357	2.79,	1.98,	1.11,	1.00,	1.93,	2.81

[a] Without any constraints in the curve fitting.
[b] Total channels = 512.

H_2. As in Fig. 5b, the outer lines corresponding to Fe^0 have disappeared. However, there are now six additional peaks, corresponding to ε′ carbide (*4*). Fitting this 28-peak spectrum, using the known peak positions of the χ-$Fe_{2.5}C$ and Fe^{2+}, gives the line positions and other parameters reported for ε′-$Fe_{2.2}C$ in Table 1.

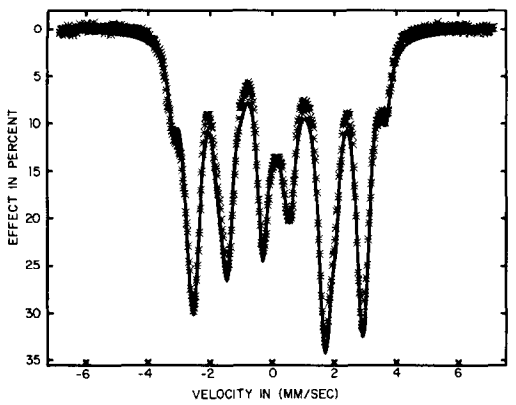

FIG. 6. Mössbauer spectrum of 10% Fe/Al_2O_3 catalyst. The reduced catalyst has been exposed to 10% CO/H_2 at 270°C for 24 h.

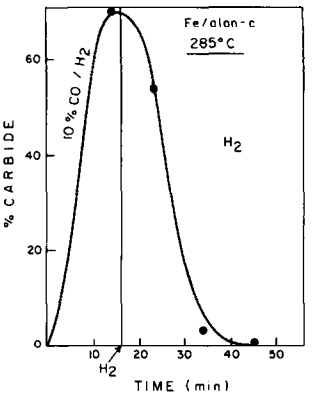

FIG. 8. Carburization and decarburization of 10% Fe/Al_2O_3.

A discussion of the fitting procedure and details of the derivation of the numerical values in Table 1 is given by Borcar *et al.* (*21*). Here we are interested only in the total carbide content as a function of time. The carburization of the iron of Fig. 6a in 10% CO/H_2 leads to a little reduction in the central Fe^{2+} peaks. However, to a good approximation the fraction of Fe^0 can be obtained simply from the relative intensities of the outer Fe^0 peaks, which are not confounded by carbide peaks. Determining the proportions of χ and ε' carbides from the spectra (*21*) is not discussed here.

Spectra like Fig. 6 were obtained at various times, and the percent carbide deduced from these measurements is plotted in Fig. 7. Figure 8 shows a similar result for 285°C and a shorter total time of exposure to 10% CO/H_2. At the end of 16 min of reaction, the extent of carburization is 70%.

The Mössbauer results are also plotted in Fig. 9 as curves 1 (285°C) and 3 (390°C) showing total carbide as a function of time of exposure to 10% CO/H_2. The other two curves (2 and 4) are obtained by mass balances and will be discussed later.

At the time indicated by the vertical line in Figs. 7 and 8 the CO/H_2 feed was replaced by H_2, leaving the reaction temperature constant. The S-shaped curves for total carbide content during decarburization correspond to peaks in the methane pro-

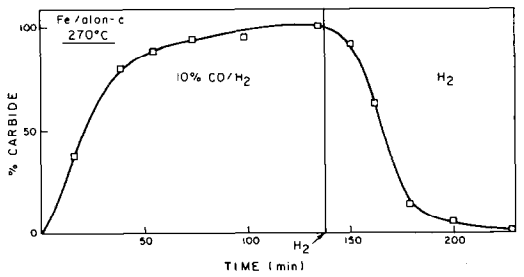

FIG. 7. Carburization and decarburization of 10% Fe/Al_2O_3 catalyst.

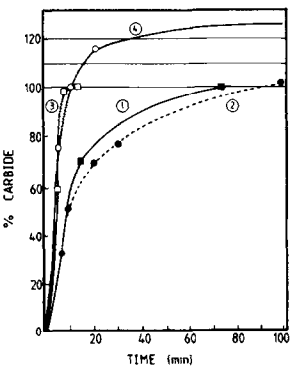

FIG. 9. Evaluation of the total carbide calculated in various ways. (1) Mössbauer measurements, 285°C. (2) Mass spectrometer measurements, 285°C; peak 3 from Table 2. (3) Mössbauer measurements, 390°C. (4) Mass spectrometer measurements, 285°C; sum of peaks 2 and 3 from Table 2.

duction rate. It is interesting that there is a long linear section for the curve of total carbide. For example, at 285°C the rate of decarburization remains about constant as the total carbide falls from 61 to 6% in 10 min. We shall use this information to interpret peaks of methane formed during decarburization in a later section.

Evolution of the Catalyst Surface and Bulk with Time Studied by Mass Spectrometry

After various times of reaction from 10 s to 1 h with a feed of 10% CO/H_2 at 285°C the feed is switched to He for 40 s and then changed to H_2. The short exposure to He is intended to remove adsorbed hydrogen. After the switch to H_2 the composition of the effluent (mostly CH_4) is recorded as a function of time. In performing a series of these experiments it is important that the catalyst always be returned to the same initial reduced state before exposure to the 10% CO/H_2 stream. For reaction times up to 2 min, a reduction in H_2 at 285°C is sufficient to restore the initial behavior. However, for longer times on stream it is necessary to reduce in H_2 at 460°C for an hour in order to regenerate the catalyst. The quantity of water removed by the helium sweep is 33 μmol/g, which is attributed to desorption from the support. Alumina dehydrated at 470°C can chemisorb about 450 μmol/g at 270°C, most of it held irreversibly. No hydrocarbons nor CO nor CO_2 are observed to desorb during the passage of the helium, but these constituents would be difficult to observe if they desorbed rapidly.

The feed gas is then switched to hydrogen. Methane, ethane, and traces of propane are then formed along with only 2 μmol/g of water. The methane formation is shown in Figs. 10 and 11. After 10 s of reaction a single sharp peak is obtained, arising from the rapid reaction of H_2 with a surface species. After 1 min of reaction a shoulder is visible on the first peak. For longer reaction times the shoulder develops into a peak; it represents a species which is less reactive to H_2 than that represented by the first peak. Starting at about the end of 1 min, a third, very flat peak is detected. The evolution of the various peaks can be followed in Figs. 10 and 11. For longer reaction times the height of the first peak slightly decreases, and that of the second rises to a maximum at an exposure time of 10 min and then falls for longer times. Except for the shortest reaction times, the maximum CH_4 production rate during the removal of the surface species is higher than the production rate from the mixture at the end of the reaction period.

Since the reaction of the surface and bulk carbonaceous species produces essentially no water, we shall assume that the surface species are CH_x and CH_y, where it is possible that y is small or zero. In what follows we discuss how we use the Mössbauer results to account for the third, flat peak as bulk carbide. The two peaks which appear

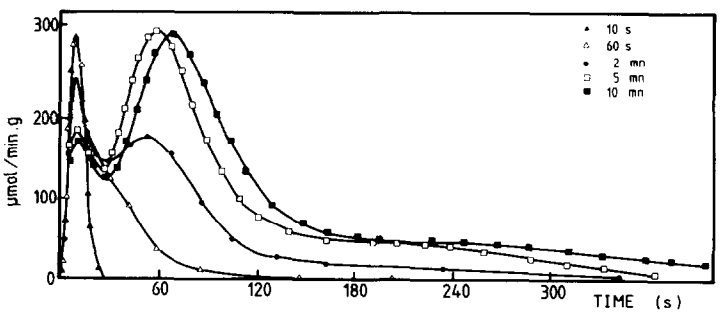

FIG. 10. Production of methane by H_2 at 285°C after various reaction times in 10% CO/H_2.

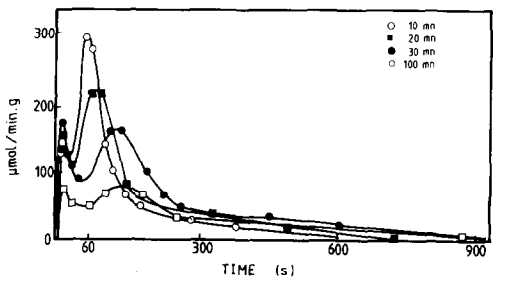

FIG. 11. Production of methane by H_2 at 285°C after various reaction times in 10% CO/H_2.

more rapidly are then associated with two more or less hydrogenated surface species.

If the surface were covered with a reactive species, say CH_x, and a less reactive species, say CH_y, we might expect that the CH_y would appear as a tail on the CH_x peak; the rate of methane production would not rise to a second maximum. For either surface species, the rate is given by an equation of the type

$$r_{CH_4} = kH^a(CH_x)^b, \qquad (1)$$

where we take a and b as unity to simplify the discussion. If CH_x covers more than half of the surface, the rate will go up to a maximum and then fall to zero as H replaces CH_x on the surface. Even if CH_x is present at less than half coverage, the finite response time of the mass spectrometer and its inlet will produce an asymmetric peak, since r_{CH_4} is zero at the start of the hydrogen flush.

If CH_y is less reactive than CH_x, it will react only slowly with H. However, as CH_x is replaced by H, (CH_y) (H) will increase, and if enough CH_y was present initially, a second maximum in r_{CH_4} will occur, as shown in Figs. 10 and 11.

The quantities of CH_4 corresponding to the three observed peaks and to three different carbonaceous intermediates are given in Table 2. The deconvolution used to obtain these quantities is shown for a typical case in Fig. 12. Separation of the first two peaks is not difficult. For the second and third peaks the MES data have been used, on the assumption that the third peak corresponds to the bulk carbide. The flat shape of this peak agrees well with rate of decarburization data which can be obtained from Fig. 8. There is a delay of about 1 min in the start of decarburization, and then between 22 and 34 min the rate of decarburization is 28 μmol/min g. This figure is based on a carbide of average composition $Fe_{2.35}C$ and a reduction of 76% of the iron. During 12 min 335 μmol/g of carbide are removed. Figures 11 and 12 show that the rates of methane production from the plateau of the third peak are in the range 25–50 μmol/min g. Thus in Fig. 12 the third peak is sketched as starting at about 50 s and then rising to the plateau value by about 80 s. By this procedure the numbers in Table 2 have been obtained. The percentage carburization is based on the carbide formula actu-

TABLE 2

Quantities of CH_4 Produced by Hydrogen at Various Reaction Times in 10% CO/H_2 at 285°C

Reaction time in 10% CO/H_2	CH_4 μmol/g of catalyst				Percentage carburization	
	Peak 1	Peak 2	Peak 3	Peak 4	Peak 3	Peak 2 + 3
10 s	49.3	0	0	0	0	0
30 s	55.3	58.4	10.3	0	1.6	11
2 min	52.9	150	95.5	0	15	40
5 min	54.0	251	205	—	33	75
10 min	51.6	309	309	—	50	101
20 min	50.6	290	426	—	69	117
30 min	52.3	226	453	50	74	111
100 min	48.2	125	630	96	102	123

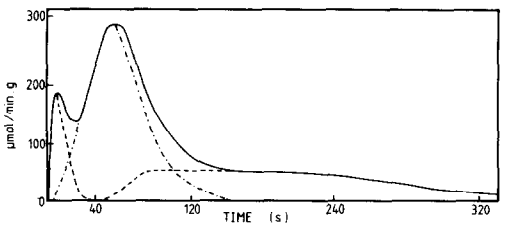

FIG. 12. Example of the deconvolution of the peaks of Figs. 10 or 11. Curves shown are for a reaction time of 5 min.

ally observed by MES at the given time. The results given in Table 2 are plotted in Fig. 9 as curves 2 and 4. Curve 2 agrees well with the MES results, especially at the lower reaction times. The sum of peaks 2 and 3 is given in Table 2 and Fig. 9 (curve 4) to show that the sum represents too much carbon to be accounted for as a bulk carbide. Since the solubility of C in α-iron is only 0.01%, this form cannot account for the observed peaks either. Thus, we conclude that our calculation of peak three as representing bulk carbide is reasonable.

The quantity of CH_4 arising from the first peak (50 μmol/g) remains about constant even as the peak maximum shown in Figs. 10 and 11 diminishes. The quantity of CH_4 corresponding to second peak reaches a maximum at about 15 min of reaction time. As time goes on, the time for peak 2 to reach its maximum increases slowly. The surface intermediate is becoming less reactive toward H_2 as time of reaction increases, either because of its own change in nature or simply because the concentration of surface hydrogen is less at the higher coverages of carbonaceous intermediates.

Having quite firmly associated the third peak with bulk carbide, the nature of the other two (surface) peaks can be considered further. The first peak is present at 50 μmol/g of catalyst. The iron surface area deduced from the physical measurements (XRD and TEM) represents about 100 μmol of iron atoms/g of catalyst. The CO adsorption, at −74°C and 2Fe/CO, represents about 126 μmol of iron/g of catalyst. Thus the first peak, at 1 Fe/CH_x involves about 0.5 times that corresponding to the physically measured area of the iron particles. If the iron sites (8.2 Å^2) could adsorb several CH_y, these smaller species (1.86 Å^2/C) could be accommodated on the area corresponding to the available sites.

To be sure that there is no accumulation of intermediates on the Al_2O_3 support, we have diluted the 10% Fe/Al_2O_3 with an equal amount of Al_2O_3 support and repeated some of the experiments. No increase in the peaks was observed.

During the time that the second peak is building up (Figs. 10 and 11) the rate of methanation (Fig. 3) is *increasing*. Thus the second species is not a poison. The maximum quantity of the second species (CH_y) is 309 μmol/g of catalyst (Table 2). There are two ways to explain this large quantity present on the restricted iron area available. This species, less reactive than the first species, may be a slightly hydrogenated carbon chain, so that it can be accommodated on about half of the metallic surface. An alternative explanation is that a number of CH_y can be associated with each iron atom as discussed above. However, no definite conclusions can be drawn without some kind of better data on the surface analysis and the location of the adsorbed species.

During the formation of methane illustrated in Figs. 10 and 11, a small peak of ethane is also detected, as shown in Fig. 13. This peak occurs under the first methane peak only and indicates that the first surface species involved may be the one which

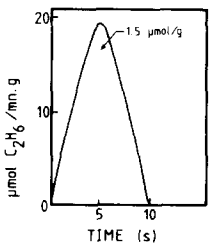

FIG. 13. Production of C_2H_6 by hydrogen at 285°C after times of reaction in 10 CO/H_2 between 40 s and 5 min.

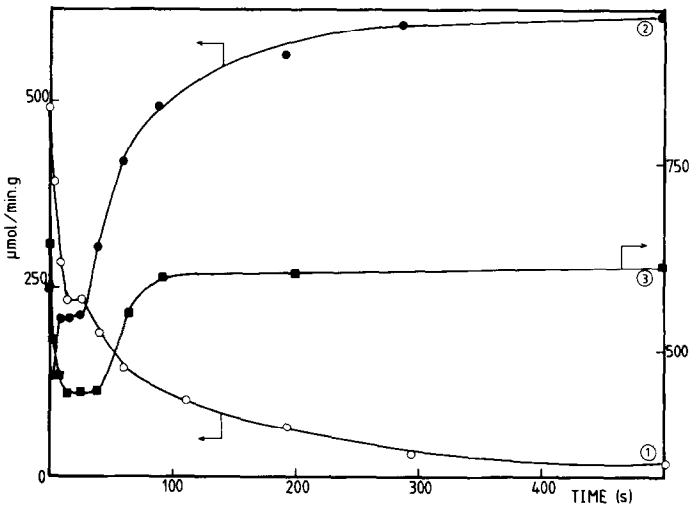

FIG. 14. Evolution of carbon in various forms during reaction of 10% CO/H_2 at 285°C. (1) Rate of carbon deposition. (2) Rate of appearance of hydrocarbons. (3) Rate of carbon monoxide dissociation. See text for the definitions of these quantities.

leads to polymerization. CH_x is probably also more hydrogenated. A trace of propane is observed with the CH_4, C_2H_6 peak.

After sufficient time in hydrogen, no further methane production is observed in the experiments of Figs. 10 and 11. The MES results show that all the carbide is also gone at this time. The feed is changed to helium and the reactor heated quickly to 460°C. The feed is then switched back to hydrogen, and for long reaction times a peak of methane is obtained, as listed in Table 2. The quantity of this hard-to-remove carbon increases with time on stream, and it is logical to associate it with graphitic (unreactive) carbon. This species is often associated with the long-term deactivation of the reaction (*6, 7*). The surface composition of iron after CO/H_2 reaction has been studied by Krebs *et al.* (*25*) using a polycrystalline foil and by Bonzel and Krebs (*6*) using the (100) face of a single crystal. The analyses were made by Auger electron spectroscopy (AES) and by x-ray photoelectron spectroscopy (XPS). For the crystal three types of carbon are proposed: a hydrogenated surface carbon, a carbidic surface carbon, and a graphitic surface carbon. It is reasonable to associate the graphitic carbon with our peak 4. Our peak 1 seems to be the precursor of higher hydrocarbons and is the most reactive toward hydrogen, so it may be the more hydrogenated species (CH_x). The peak 2, less reactive and probably less hydrogenated (CH_y), we may associate with the carbidic carbon of Ref. (*6*).

Material Balance on Deposited Carbon

The total quantity of carbon incorporated onto the surface and into the bulk of the catalyst can be calculated from the data like those of Figs. 3 and 4 but obtained at 285°C. At any particular time during the reaction we have the following rates (μmol/g · min):

(1) Carbon deposited = $CO_{in} - CO_{out} - CO_2$ – (2)

(2) Carbon in hydrocarbon products = $CH_4 + 2C_2H_6 + 3C_3H_8 + 4C_4H_{10}$

(3) Total carbon monoxide dissociated = (1) + (2) = $CO_{in} - CO_{out} - CO_2$.

The results of this calculation appear in Fig. 14 for the first 10 min of reaction. The reliability of the procedure can be evaluated by comparing the total amount of carbon obtained by integrating curve 1 of Fig. 14 up to the appropriate time with the amount corresponding to the sum of peaks 1 through 4 of Table 2. The results are given

TABLE 3

Material Balance on Carbon Deposited during Reaction in 10% CO/H_2 at 285°C

Reaction time in 10% CO/H_2	Sum of peaks 1–3, Table 2 (μmol/g)	Integration under curve b of Fig. 14
10 s	49.3	59.7
30 s	124	137
2 min	298[a]	351
5 min	510[a]	551

[a] These figures should be increased by peak 4 (unreactive carbon), not measured.

in Table 3, and the agreement is satisfactory.

An interesting feature of Fig. 14 is that the rate of CO dissociation goes through a minimum at 10–40 s and then remains almost constant at about 612 μmol/g min from 100 s onward. During the latter period the rate of hydrocarbon production is slowly increasing mainly because the rate of incorporation of carbon onto and into the catalyst is decreasing.

From Table 2 and Fig. 14 it is calculated that during the first 10 s of reaction the entire first peak is rapidly formed at about 300 μmol/g min average rate. Then between 10 and 30 s most of the carbon goes into the second peak, at about 180 μmol/g min average rate. This rate then decreases until it becomes zero at about 10 min, after which peak 2 starts to decrease. During the time after about 1 min the carburization rate is of the order of 40 μmol/g min.

CONCLUSIONS

By using mass spectrometry and Mössbauer effect spectroscopy it has been possible to determine the evolution of the surface and bulk compositions of a 10% Fe/Al_2O_3 precipitated catalyst after the catalyst, reduced in H_2 at 460°C, is exposed to 10% CO/H_2 at 285°C. Initially the well reduced iron shows a very high methanation activity which decreases rapidly as the iron surface is covered with 50 μmol/g of surface species 1 in the first 10 s of reaction. Then a second surface species starts to build up, and the methanation rate increases again as this species 2 increases to a maximum. Carbide builds up more slowly than the two surface species and probably has less effect on the reaction rates. The hydrocarbon production rate increases up until about 30 min at 270°C, or 10 min at 285°C. This change is not associated with a higher rate of CO dissociation. On the contrary, the latter changes little after 1 min of reaction time. As the reaction rate goes up, the rate of accumulation of surface carbonaceous species decreases by an equivalent amount (Fig. 14). Finally the surface starts to accumulate inert graphite-like carbon, and the rate decreases slowly. Water is found to be a reversible inhibitor of the rate, probably by reducing the surface hydrogen coverage.

The data in this paper give a picture of the evolution of the catalyst as reaction proceeds. We have not discussed the chemical composition of the surface species 1 and 2, other than to note that they are probably CH_x and CH_y. No appreciable water is formed during the hydrogenation of the surface, so no oxygen seems to be involved. These matters will be considered in a future paper.

ACKNOWLEDGMENT

We express our appreciation to the National Science Foundation for the financial support of this work through Grants ENG 7821890 and CPE81-20499. Some of the chemisorption measurements were made by L. M. Tau and E. DiMattia. We also appreciate several useful discussions with Professor S. J. Teichner of the University of Lyon.

REFERENCES

1. Amelse, J. A., Butt, J. B., and Schwartz, L. H., *J. Phys. Chem.* **82,** 558 (1978).
2. Raupp, G. B., and Delgass, W. N., *J. Catal.* **58,** 337, 348, 361 (1979).
3. Matsumoto, H., and Bennett, C. O., *J. Catal.* **53,** 331 (1978).
4. Niemantsverdriet, J. W., van der Kraan, A. M., van Dijk, W. L., and van der Baan, H. S., *J. Phys. Chem.* **84,** 3363 (1980).

5. Nahon, Nicole, thesis, Lyon, 1979.
6. Bonzel, H. P., and Krebs, H. J., *Surf. Sci.* **91,** 499 (1980).
7. Dwyer, D. J., and Somorjai, G. A., *J. Catal.* **52,** 291 (1978).
8. Dumesic, J. A., Topsoe, H., and Boudart, M., *J. Catal.* **37,** 513 (1975).
9. Bianchi, D., Batis-Landoulsi, H., Bennett, C. O., Pajonk, G. M., Vergnon, P., and Teichner, S. J., *Bull. Soc. Chim. Fr.* **I,** 345 (1981).
10. Blyholder, G., and Neff, L. D., *J. Phys. Chem.* **66,** 1664 (1962).
11. Anderson, J. R., "Structure of Metallic Catalysts." Academic Press, New York, 1975.
12. Vannice, M. A., *J. Catal.* **37,** 449 (1975).
13. Brenner, A., and Hucul, D. A., *Inorg. Chem.* **18,** 2836 (1979).
14. Amelse, J. A., Schwartz, L. H., and Butt, J. B., *J. Catal.* **72,** 95–110 (1981).
15. Emmett, P. H., and Harkness, R. W., *J. Amer. Chem. Soc.* **57,** 1631 (1935).
16. Jung, H-J., Vannice, M. A., Mulay, L. N., Stanfield, R. M., and Delgass, W. N., *J. Catal.* **766,** 208–224 (1982).
17. Boudart, M., Delbouille, A., Dumesic, J. A., Khammouma, S., and Topsoe, H., *J. Catal.* **37,** 486 (1975).
18. Solbakken, V., Solbakken, A., and Emmett, P. H., *J. Catal.* **15,** (1969).
19. Wilson, W., and Schwartzendruber, L. J., *Comp. Phys. Commun.* **7,** 151 (1974).
20. Delgass, W. M., and Chen, L. Y., *Rev. Sci. Instrum.* **47,** 968 (1976).
21. Borcar, S., Tau, L. M., Bianchi, D., and Bennett, C. O., submitted for publication.
22. Blanchard, Francoise, thesis, Lyon, 1981.
23. Reymond, J. P., Mériaudeau, P., Pommier, B., and Bennett, C. O., *J. Catal.* **4,** 163 (1980).
24. Nijs, H. H., and Jacobs, P. A., *J. Catal.* **66,** 401 (1980).
25. Krebs, H. J., Bonzel, H. P., and Gafner, G., *Surf. Sci.* **88,** 269–283 (1979).